

# Geometric and electronic structure of carbon nanotube networks: ‘super’-carbon nanotubes

V R Coluci<sup>1</sup>, D S Galvão<sup>1</sup> and A Jorio<sup>2</sup>

<sup>1</sup> Instituto de Física ‘Gleb Wataghin’, Universidade Estadual de Campinas, CP 6165, 13083-970 Campinas SP, Brazil

<sup>2</sup> Departamento de Física, Universidade Federal de Minas Gerais, Belo Horizonte, MG, 30123-970, Brazil

E-mail: [coluci@ifi.unicamp.br](mailto:coluci@ifi.unicamp.br)

Received 9 September 2005, in final form 4 November 2005

Published 6 January 2006

Online at [stacks.iop.org/Nano/17/617](http://stacks.iop.org/Nano/17/617)

## Abstract

Structures of the so-called super-carbon nanotubes are proposed. These structures are built from single walled carbon nanotubes connected by Y-like junctions forming a ‘super’-sheet that is then rolled into a seamless cylinder. Such a procedure can be repeated several times, generating a fractal structure. This procedure is not limited to carbon nanotubes, and can be easily modified for application to other systems. Tight binding total energy and density of states calculations showed that the ‘super’-sheets and tubes are stable and predicted to present metallic and semiconducting behaviour.

(Some figures in this article are in colour only in the electronic version)

## 1. Introduction

Carbon based materials present an enormous variety of forms and properties. Among these structures are graphite, diamond, fullerenes, and carbon nanotubes [1–3]. A single walled carbon nanotube (SWNT) can be considered heuristically as formed by rolling up a graphene sheet to make a seamless cylinder. Due to the extreme mechanical and thermal properties related to the strong carbon–carbon bonding, and the interesting electronic properties related to the quantum confined structure, they will play an important role in the development of nanotechnology [4].

Junctions among SWNTs can be produced by introducing pentagon–heptagon pair defects into the hexagonal network inducing changes in the electronic properties [5]. Two SWNTs can be welded by electron beam exposure at high temperatures resulting in ‘X’-, ‘Y’-, or ‘T’-like stable junctions induced by structural defects created during the beam irradiation [6, 7]. This type of arrangement opens up the possibility of creating carbon nanotube networks [8, 9]. Two-dimensional superstructures of honeycomb symmetry have been proposed and shown to be interesting in terms of superconductivity [10]. Furthermore, three-dimensional nets using fullerene forms with seven- or eight-membered

rings have been predicted to present a variety of electronic properties [11].

In this work we propose new structures generated from a carbon network based on the honeycomb symmetry. The starting structure, generically named the super-graphene (SG), is heuristically constructed, replacing the carbon–carbon bonds of the graphene architecture by SWNTs, and the carbon atoms by Y-like junctions. From the super-graphene a new tubular structure can be generated. We named this tubular structure *super-nanotube* (ST) which represents a carbon nanotube made of carbon nanotubes.

## 2. Construction of super-carbon nanotubes

The construction of a ST can be viewed as a process analogous to the one used to generate SWNTs. The initial point is the graphene sheet (figures 1(a) and (b)) which is rolled up to construct a SWNT (figure 1(c)). For the ST case, the super-graphene is initially built (figures 1(d) and (e)) connecting SWNTs through the use of Y-junctions. Finally, the super-tube is produced by wrapping the super-graphene sheet (figure 1(f)). Similarly to a  $(n, m)$  SWNT [3],  $(N, M)$  ST with different chiralities can be constructed. These superstructures (SG

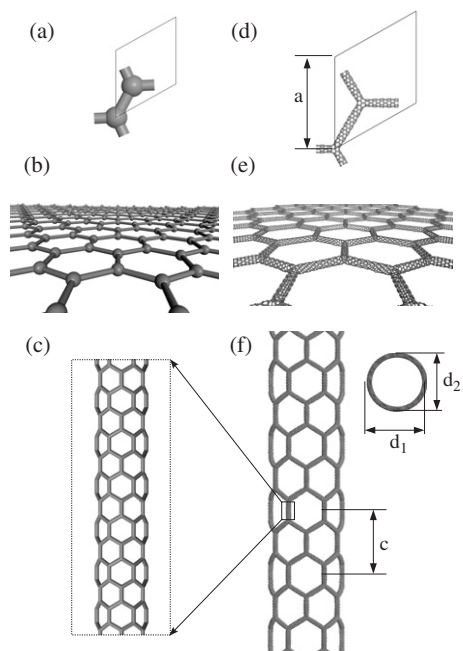


**Figure 1.** Schematic view of the process used to generate a SWNT, (a)–(c), and a ST, (d)–(f). Representation of the (a) graphene sheet and (b) super-graphene unit cells. The sheets (b) and (e) are then rolled up to form a (c) SWNT and a (f) ST, respectively. The parameters  $a$ ,  $c$ ,  $d_1$ , and  $d_2$  characterize the superstructures. The SWNT (c) is used to construct the ST shown in (f).

and ST) are characterized by the SWNT used to form their sides, its length (parameters  $a$  and  $c$ ; figure 1), and the necessary junctions for joining consecutive tubes. The super-tube construction is not limited to carbon nanotubes and to the honeycomb symmetry, and represents a three-dimensional network of nanotubes. It can be applied to other tubular structures such as boron nitride nanotubes and to different symmetries through the use of other junction types (X- or T-junctions, for example). Due to the size and properties of such tubes, many applications can be imagined for them, from catalytic sites for reactions of large biomolecules to high strength composites and actuators.

We define the super-graphene made by connecting  $(n, m)$  SWNTs as  $SG@(n, m)$ . The unit cell of the SGs presents a hexagonal symmetry having the lattice vectors  $(0, a)$  and  $(\sqrt{3}a/2, a/2)$  (figure 1(d)). A super-nanotube is represented as  $[N, M]@(n, m)$  which has an  $(N, M)$  structure and is formed from  $(n, m)$  SWNTs. Two metallic  $((6, 0)$  and  $(3, 3))$  and one semiconducting SWNT  $((8, 0))$  were used here to create SGs and STs. These tubes were connected using proper junctions constructed using 5- and 7- [12] and 5- and 8-membered rings [13] for metallic and semiconducting SWNTs, respectively. However, different combinations can be used through different types of SWNTs depending on the junction type [12]. For instance, a hybrid SG made of  $(6, 0)$  and  $(3, 3)$  SWNTs ( $SG@(6, 0) (3, 3)$ ) can be generated using a mixed junction which connects them. The first property of the STs which we can point out is the presence of large pores on the sidewalls. The size of these pores is comparable to the typical size of proteins ( $\sim 5$ – $20$  nm). This property might make possible the use of STs as cavities

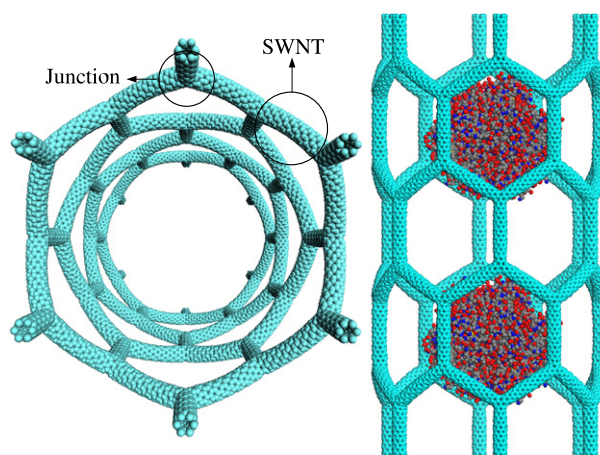


**Figure 2.** Atomistic views of a super-carbon nanotube  $[6, 0]@(6, 0)$ . On the right the super-tube contains two deoxyhaemoglobin molecules which resemble, on a different size scale, carbon nanopeapods [18].

and reservoirs, protein delivery, and allow crystallographic studies of the properties of large biomolecules which are difficult to crystallize. Atomistic views of a ST are shown in figure 2. Furthermore, electromechanical actuation should be very efficient for the STs, mainly along the axial direction, since they present a large surface area for collecting charges (doping) and a preferential alignment of the SWNTs along that direction due to the hexagonal symmetry.

### 3. Methodology

Due to the size of the structures analysed here ( $\sim 300$ – $4500$  atoms in the unit cell) which precludes the use of first principles methods, we applied a tight binding approach to determine the structural stability and the electronic properties of the SGs and STs. We have used the tight binding model by Porezag *et al* [14] implemented in the Trocadero program [15]. This model includes explicitly the non-orthogonality of the  $s$ – $p$  basis, in which the hopping matrix elements are obtained directly from density functional theory calculations using the same basis set but disregarding three-centre contributions to the Hamiltonian. This method has been successfully applied to the prediction of allotropic forms of carbon [16] and has been proven to combine accuracy and reduced computational effort, especially for large systems. The use of the  $\Gamma$  point for the Brillouin-zone sampling has been shown to be sufficient for the total energy convergence for the superstructures considered here. The geometries used in tight binding calculations were obtained by relaxing the structures (both atomic positions and cell parameters) using the universal force field [17] which includes van der Waals, bond stretch, bond angle bend, and torsional rotation terms. We have used the following relaxation convergence criteria: maximum atom force of  $0.5 \text{ kcal mol}^{-1} \text{ \AA}^{-1}$ , energy differences of  $0.001 \text{ kcal mol}^{-1}$ , maximum atomic displacement of  $0.015 \text{ \AA}$ , and root mean square displacement of  $0.003 \text{ \AA}$ .

### 4. Results

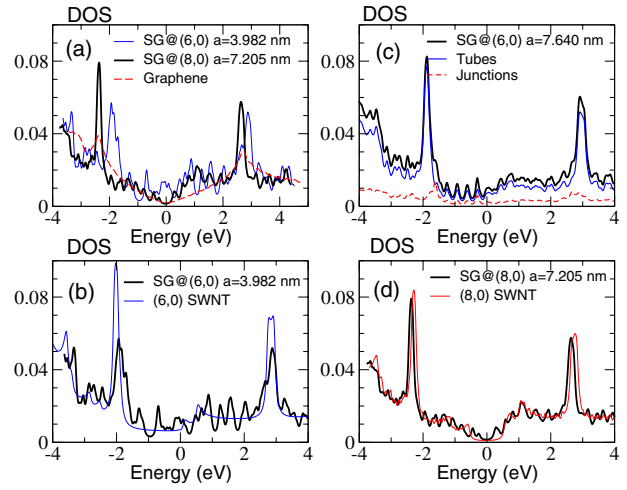
Table 1 presents the energetic properties and the size dimensions of the superstructures considered in this work.

**Table 1.** Total energy per atom with respect to graphene ( $E_T$ ), number of atoms in the unit cell ( $N_a$ ), and the size of super-graphenes and super-tubes.

| Structure       | $E_T$ (eV) | $N_a$ | Size (nm)                           |
|-----------------|------------|-------|-------------------------------------|
| SG@(8, 0)       | 0.267      | 504   | $a = 4.276$                         |
|                 | 0.249      | 888   | $a = 7.205$                         |
| SG@(6, 0)       | 0.504      | 364   | $a = 3.982$                         |
|                 | 0.461      | 508   | $a = 5.457$                         |
|                 | 0.441      | 724   | $a = 7.640$                         |
|                 | 0.431      | 868   | $a = 9.098$                         |
| SG@(3, 3)       | 0.546      | 444   | $a = 5.427$                         |
|                 | 0.541      | 768   | $a = 9.214$                         |
| [4, 0]@(8, 0)   | 0.335      | 4032  | $c = 7.690,$<br>$d_1 = d_2 = 5.80$  |
| [4, 4]@(8, 0)   | 0.293      | 4032  | $c = 4.278,$<br>$d_1 = d_2 = 10.03$ |
| [6, 0]@(6, 0)   | 0.508      | 4368  | $c = 6.950,$                        |
|                 |            |       | $d_1 = 8.15, d_2 = 7.65$            |
| [6, 6]@(6, 0)   | 0.493      | 4368  | $c = 3.991,$<br>$d_1 = d_2 = 13.76$ |
| (8, 0)          | 0.215      | 32    | $c = 0.422$                         |
| (6, 0)          | 0.393      | 24    | $c = 0.420$                         |
| (3, 3)          | 0.524      | 12    | $c = 0.243$                         |
| C <sub>60</sub> | 0.477      | 60    | —                                   |

For comparison the values for C<sub>60</sub>, and (8, 0), (6, 0), (3, 3) SWNTs are also shown. As expected (due to the presence of junctions) in relation to their corresponding SWNTs the superstructures have a higher total energy per atom. The use for instance of a supra-molecular synthetic approach (using tubes already formed) makes this aspect less limiting. The values indicate that the superstructures are stable and, in some cases, even more stable than the C<sub>60</sub>. As expected, increasing the side of the hexagon ( $a$  value) in the SGs, an increase in the stability can be observed, due to the decrease in the contribution of the structural deformation presented in the junction region to the total energy of the structure. We can see that the superstructures made by (8, 0) SWNTs are more stable than the ones constructed using (6, 0) and (3, 3) tubes. This can be associated with the lower strain energy ( $E_T^{\text{tube}} - E_T^{\text{sheet}}$ ) presented by (8, 0) SWNTs and to the use of pentagon–octagon pair defects which reduces the structural deformation. The STs [4, 0]@(8, 0) and [4, 4]@(8, 0) were generated from SG@(8, 0) with  $a = 4.276$  nm, while the [6, 0]@(6, 0) and [6, 6]@(6, 0) were from SG@(6, 0) with  $a = 3.982$  nm. An elliptical cross section ( $d_1/d_2 \simeq 1.06$ ) was obtained for the [6, 0]@(6, 0) while a circular one was found for the other super-tubes considered here. This is associated with distortions of the SWNT diameter close to the junction. These distortions are larger for SWNTs with small diameters (e.g. (6, 0)), causing an internal stress in the ST structure. The stress is released by producing a non-circular cross section. Increasing the ST diameter or considering larger SWNTs (e.g. (8,0)) for the construction of STs will cause  $d_1/d_2 = 1$ . The strain energy necessary to form the tube from the parent sheet is about 100 times smaller for the STs in comparison to the (8, 0) and (6, 0) SWNTs. This aspect can be associated with the high flexibility presented by SWNTs [19] which allows the bending of the super-graphene sheet to form the super-tube with a small energy cost.

Figure 3 presents the electronic density of states (DOS) of some of the SGs considered in this work. For comparison the

**Figure 3.** Electronic density of states (DOS) of the super-graphenes. In all DOS plots the Fermi level is positioned at zero energy and the DOS unit is number of states per eV normalized by the total number of states.

DOS of the graphene and SWNTs are also shown. The general profile of the SGs DOS is very different from the graphene one (figure 3(a)) but is dictated by the DOS of the infinite SWNTs which are used to construct them (figures 3(b)–(d)). The detailed DOS structure, however, depends on  $(n, m)$ , as well as the nanotube lengths. In figures 3(b) and (c) one can see that the SGs considered here can exhibit a metallic behaviour, like the  $(n, m)$  used to build them. Interestingly, many peaks can be observed, showing the appearance of many electronic bands close to the Fermi level. The DOS for the SG is more spiky, exhibiting sharp peaks at energies where the DOS for the SWNT is smooth, which would lead to important differences in their optical properties [20]. Furthermore, on increasing the unit cell size, i.e., by increasing the length of the SWNT which composes the SG, some changes are observed in the DOS (compare thick solid lines on figures 3(b) and (c)). These DOS changes suggest the presence of quantization effects along the nanotube length due to the formation of the new super-periodic structure. The role of the junctions is shown in figure 3(c), and it is basically to add a background into the DOS of the tube contribution to the total DOS of the SG. In the limit  $a \rightarrow \infty$  the junction contribution is expected to be almost zero in the DOS of the SGs. While the semiconducting behaviour of the (8, 0) SWNT is preserved in the SG@(8, 0) (figure 3(d)), new peaks appear and the bandgap is lowered.

Figure 4 presents the DOS of the super-tubes considered in this work. Figures 4(a) and (b) show the DOS for semiconducting and metallic super-tubes, respectively. As mentioned before, many types of network are possible depending on the kind of junction used to build them. In the present work we limited ourselves to discussing the cases where the ‘super-’nanotube structures and the ‘normal’ nanotube structures share the main electronic features (metallic/semiconducting). Despite the general electronic profile being defined by the SWNT which forms the ST, both STs chiralities (through  $[N, M]$ ) and constituents (through  $(n, m)$ ) lead to evident differences in the DOS. Similarly to the SG case, many spikes appear in the DOS of STs when



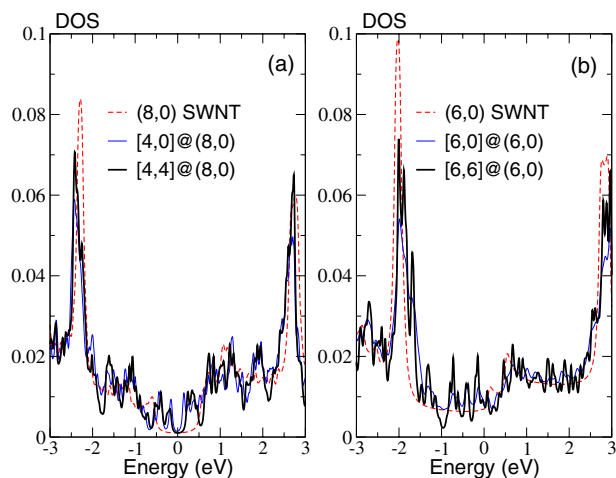


**Figure 4.** Electronic density of states of the super-tubes considered in this work.

compared to the DOS for the infinite SWNTs. Furthermore, the ST, as well as the SG structure, presents properties which are different from those of its constituents as shown in figure 4(a). In this case the STs present a smaller bandgap ( $\sim 0.2\text{--}0.4$  eV) in comparison to its equivalent SWNT value ( $\sim 1.0$  eV). The more asymmetrical valence and conduction bands of ST in comparison with the case of the SWNT is a consequence of the presence of the junctions lowering the symmetry of the ST in comparison with their related SWNTs. These results are suggestive of many possibilities for the electronic structure of these superstructures, obtained by changing  $[N, M]$ ,  $(n, m)$ , nanotube lengths, junctions or even mixing different  $(n, m)$  SWNTs within the same ST. In the present work we limited ourselves to the study of achiral structures due to computational costs but the results for the chiral ones are expected to be similar.

Besides the electronic features, the mechanical properties of STs are also expected to show interesting aspects. Since they are constructed with SWNTs, high flexibility for bending and high tensile strength are expected. The arrangement of SWNTs in networks through the use of junctions can significantly change the mechanical properties in comparison with those of the isolated SWNTs. For example, during an axial tensile straining in a ST based on the honeycomb architecture, a change in the angles of the junction can occur before the SWNTs begin to be stretched, leading to a higher value of the ultimate tensile strength. Studies along this direction are in progress. Furthermore, the large separation between the SWNTs would make difficult the formation of ST bundles, unlike in the SWNT case.

The procedure for constructing a ST can be generalized to produce higher order STs. In this sense a SWNT can be considered as the ST of the lowest order ( $ST^{(0)}$ ), being the building block for the next order ( $ST^{(1)}$ ). A ST of order  $k$  can be recursively made of STs of the previous order  $k - 1$  ( $ST^{(k-1)} \rightarrow ST^{(k)}$ ) since the initial step of the generation rule is known:  $ST^{(0)} \rightarrow ST^{(1)}$ . This aspect is illustrated in figure 5.

The methods of synthesis of the superstructures are the key remaining and currently challenging issues. Progress in synthesis of one specified type of SWNT is also needed

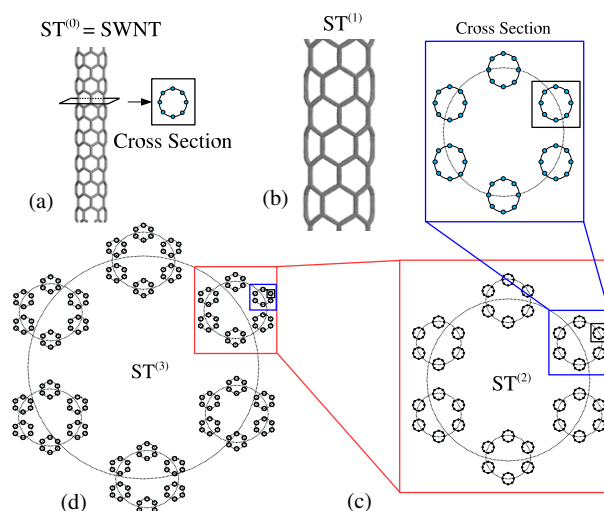


**Figure 5.** Schematic view of the fractal generation of higher order STs. In (a) the cross section of a SWNT is shown where the bonds are represented by small circles. (b) The  $ST^{(1)}$  cross section is shown. (c) The  $ST^{(2)}$  is constructed from  $ST^{(1)}$ , (d)  $ST^{(3)}$  from  $ST^{(2)}$ , and so on.

to allow the production of the pure ST. Baughman *et al* have proposed a strategy based on topochemical reactions which can lead to the synthesis of specific SWNTs [21]. Recent advances in the controlled fabrication of hierarchically branched nanotubes have been made using porous templates and could help in the production of structures of greater topological complexity [22]. Another approach for the production of STs would be to grow SWNTs inside templates with the super-nanotube structure, similar to the growth of 0.4 nm SWNTs [23] and Y-junctions [24], or to explore the ability of biological macromolecules to assemble into a wide variety of complex functional structures and coat carbon nanotubes [25]. Complex DNA structures have been already produced using such ability [26]. Also, Huang *et al* have recently demonstrated that nanotube networks can be built by sequential controlled placement [27]. These results represent a significant advance towards super-carbon nanotube realization.

## 5. Conclusion

In summary, new carbon structures forming networks are proposed. They are based on the graphene architecture where the carbon bonds are replaced by single walled carbon nanotubes, and the carbon atoms by Y-like junctions of three single walled carbon nanotubes (super-graphene). A super-carbon nanotube can be formed from this network by wrapping it in a similar way to what has been done for usual carbon nanotubes. These super-tubes can present either metallic or semiconducting behaviour, be prototypes for electromechanical actuators, and serve as hosts for large biomolecules. The richness of their electronic structure shows here a concept for forming a periodic superstructure from basic nanoscopic components. We hope the present study will stimulate further experimental studies for synthesizing such structures.

## Acknowledgments

We gratefully thank S O Dantas, R Rurali, and E Hernandez for helpful discussions regarding the Trocadero program, and M S Dresselhaus, R Saito, and Ge G Samsonidze for critically reviewing the manuscript. We also acknowledge financial support from the Instituto de Nanociências and IMMP/CNPq, the Brazilian agencies FAPESP, Capes, CNPq, and the use of computational facilities at CENAPAD-SP.

## References

- [1] Iijima S 1991 *Nature* **354** 56
- [2] Saito R *et al* 1992 *Chem. Phys. Lett.* **195** 537
- [3] Saito R, Dresselhaus G and Dresselhaus M S 1998 *Physical Properties of Carbon Nanotubes* (London: Imperial College Press)
- [4] Baughman R H *et al* 2002 *Science* **297** 787
- [5] Chico L *et al* 1996 *Phys. Rev. Lett.* **76** 971
- [6] Terrones M *et al* 2002 *Phys. Rev. Lett.* **89** 075505
- [7] Biro L P *et al* 2004 *Diamond Relat. Mater.* **13** 241
- [8] Terrones M 2003 *Annu. Rev. Mater. Res.* **33** 419
- [9] Dag S *et al* 2004 *Phys. Rev. B* **70** 205407
- [10] Shima N and Aoki H 1993 *Phys. Rev. Lett.* **71** 4389
- [11] Fujita M *et al* 1995 *Synth. Met.* **71** 1897
- [12] Zsoldos I *et al* 2004 *Mod. Sim. Mater. Sci. Eng.* **12** 1251
- [13] Srivastava D *et al* 1998 *Ann. New York Acad. Sci.* **852** 178
- [14] Porezag D *et al* 1995 *Phys. Rev. B* **51** 12947
- [15] Rurali R and Hernandez E 2003 *Comput. Mater. Sci.* **28** 85
- [16] Terrones H *et al* 2000 *Phys. Rev. Lett.* **84** 1716
- [17] UFF-Universal1.02 Molecular Force Field, available from Accelrys, Inc. in Cerius2 program <http://www.accelrys.com>
- [18] Smith B W *et al* 1998 *Nature* **396** 323
- [19] Iijima S *et al* 1996 *J. Chem. Phys.* **104** 2089
- [20] Jorio A *et al* 2004 *MRS Bull.* **29** 276
- [21] Baughman R H *et al* 2004 *Synth. Met.* **141** 87
- [22] Meng G *et al* 2005 *Proc. Natl Acad. Sci.* **102** 7074
- [23] Wang N, Li G D and Chen J S 2000 *Nature* **408** 50 (doi:10.1038/35040702)
- [24] Li J, Papadopoulos C and Xu J 1999 *Nature* **402** 253
- [25] Dalton A B *et al* 2004 *Adv. Funct. Mater.* **14** 1147
- [26] Shih W M *et al* 2004 *Nature* **427** 618
- [27] Huang X M H *et al* 2005 *Nano Lett.* **5** 1515